Electronic Supplementary Information

Well-dispersed bi-component-active $CoO/CoFe_2O_4$ nanocomposites with tunable performances as anode materials for lithium-ion batteries

Xiamei Li,[a] Yaxia Yin,[bc] Congju Li,[b] Fazhi Zhang,[a] Li-Jun Wan,[c] Sailong Xu*[a] and David G. Evans[a]

[a] State Key Laboratory of Chemical Resource Engineering, Beijing University of Chemical Technology, Beijing 100029, China; Email: xusl@mail.buct.edu.cn

[b] College of Materials Science and Engineering, Beijing University of Chemical Technology, Beijing 100029, China

[c] Beijing National Laboratory for Molecular Sciences, Institute of Chemistry, Chinese Academy of Sciences (CAS), Beijing 100090, China.

Experimental

Materials All chemicals were used without further purification, involving $Co(NO_3)_2{\cdot}6H_2O$, $Fe(NO_3)_3{\cdot}9H_2O$, $Fe(NO_3)_2{\cdot}6H_2O$, and CoO (from Alfa Aesar China (Tianjin) Chem. Co., Ltd.), as well as Na_2CO_3 and NaOH (from Beijing Chem. Co., China).

Preparation of CoFe-LDH Precursor CoFe-LDH precursors were prepared by using a scalable procedure of separate nucleation and aging steps (SNAS) in a modified colloid mill reactor.[1-3] A salt solution were obtained by dissolving $Co(NO_3)_2{\cdot}6H_2O$ and $Fe(NO_3)_3{\cdot}9H_2O$ with different Co/Fe molar ratios of 3:1 and 2:1 in freshly deionized water to give a solution with a total cationic concentration of 1.2 M, and a aqueous base solution of NaOH (1.92 M) and Na_2CO_3 (0.8 M) was also obtained. Equal volumes of salt and base solutions were simultaneously added into a modified colloid mill with a rotor speed set at 3000 rpm, and the resulting slurry was

mixed for 1 minute. The resulting slurry was aged at 80 °C for 48 h, then washed thoroughly with deionized water by centrifugation, and finally dried at 60 °C for 24 h. Also, for preparing the control materials of pristine $CoFe_2O_4$, the $CoFe^{2+}Fe^{3+}$-LDH precursor was prepared under the same conditions except for a $Co/Fe^{2+}/Fe^{3+}$ molar ratio of 1:1:1 in accordance with our recent study.[3]

Preparation of $CoO/CoFe_2O_4$ Nanocomposites and Control Materials Calcination of the CoFe-LDH precursors was performed in a fused quartz tube mounted in a programmable tube furnace. The LDH precursors were heated in flowing helium to the desired temperature at 700 °C at a temperature ramping rate of 2 °C/min, kept at temperature for 2 h, and then cooled to ambient temperature. The products were denoted as $5CoO/CoFe_2O_4$ and $3CoO/CoFe_2O_4$, respectively, on the basis of the theoretic molar ratios (5:1 and 3:1) of $CoO/CoFe_2O_4$ after the conversion from the CoFe-LDH precursor (Co/Fe molar ratios of 3:1 and 2:1) to the resultant composites. The control materials were used involving commercially available CoO, the pure $CoFe_2O_4$ derived by the above $CoFe^{2+}Fe^{3+}$-LDH precursor, and the mechanically mixed $CoO/CoFe_2O_4$ with a 5:1 molar ratio (denoted as $m5CoO/CoFe_2O_4$). Also, a low-temperature calcination was performed on the CoFe-LDH precursor with a Co/Fe molar ratio of 3:1 under the same conditions except for at 300 °C.

Characterizations Powder XRD data were recorded on a Rigaku XRD-6000 powder diffractometer with CuKα radiation (40 kV, 30 mA, λ=1.542 Å). Scanning electron microscope (SEM) images were obtained using a Zeiss Supra 55 scanning electron microscope. Elemental analysis for metal ions was performed using a Shimadzu inductively coupled plasma emission spectrometer (ICP-ES). Solutions were prepared by dissolving the sample in dilute hydrochloric acid (1:1). High-resolution transmission electron microscopy (HRTEM) image was obtained from a JEOL JEM-2100 electron microscope at an accelerating voltage of 200 kV.

Electrochemical measurements[4] were performed with Swagelok-type cells assembled in an argon-filled glove box. For preparing working electrodes, a mixture of active material, super-P acetylene black, and poly(vinyl difluoride) (PVDF) at a weight ratio of 70:20:10 was pasted on a Cu foil. Lithium foil was used as the counter

electrode. A glass fiber (GF/D) from Whatman was used as a separator. The electrolyte consisted of a solution of 1M $LiPF_6$ salt in ethylene carbonate (EC)/dimethyl carbonate (DMC)/diethyl carbonate (DEC) (1:1:1 in wt%) plus 2 wt% vinylene carbonate (VC) obtained from Tianjing Jinniu Power Sources Material Co. Ltd.. Galvanostatic cycling of the assembled cells was carried out using LAND CT2100A cell-testing system in the voltage range of 0.01–3.0 V (vs. Li^+/Li) as reported previously.[5-8] Cyclic voltammograms (CVs) were performed an electrochemistry work station (CHI 733d) at a scan rate of 0.1mv s^{-1} in the voltage range of 0– 3.0 V (vs. Li^+/Li). Electrochemical impedance spectra (EIS) were recorded over the frequency range between 100 KHz and 0.1 Hz at open circuit potential using on a Parstat 2273 advanced electrochemical system.

References

1. Y. Zhao, F. Li, R. Zhang, D. G. Evans, X. Duan, *Chem. Mater*., 2002, **14**, 4286.
2. S. L. Xu, Z. Chen, B. Zhang, J. Yu, F. Z. Zhang, D. G. Evans, *Chem. Eng. J*., 2009, **155**, 881.
3. S. L. Xu, Y. Yang, T. Xu, Ye. Kuang, M. Dong, F. Z. Zhang, F. Besenbacher, D. G. Evans, *Chem. Eng. Sci.*, 2011, **66**, 2157.
4. Y.-X. Yin, S. Xin, L.-J. Wan, C.-J. Li, Y.-G. Guo, *J. Phys. Chem. C*, 2011, **115**, 14148.
5. P. Poizot, S. Laruelle, S. Grugeon, L. Dupont, J-M. Tarascon, *Nature*, 2000, **407**, 496.
6. Y.-Q. Chu, Z.-W. Fu, Q.-Z. Qin, *Electrochim. Acta,* 2004, **49**, 4915.
7. J. Cabana, L. Monconduit, D. Larcher, M. R. Palacín, *Adv. Mater.,* 2010, **22**, E170.
8. J. X. Zhu, Y. K.r Sharma, Z. Y. Zeng, X. J. Zhang, M. Srinivasan, S. Mhaisalkar, H. Zhang, H. H. Hng, Q. Y. Yan, *J. Phys. Chem. C,* 2011, **115**, 8400.

Fig. S1

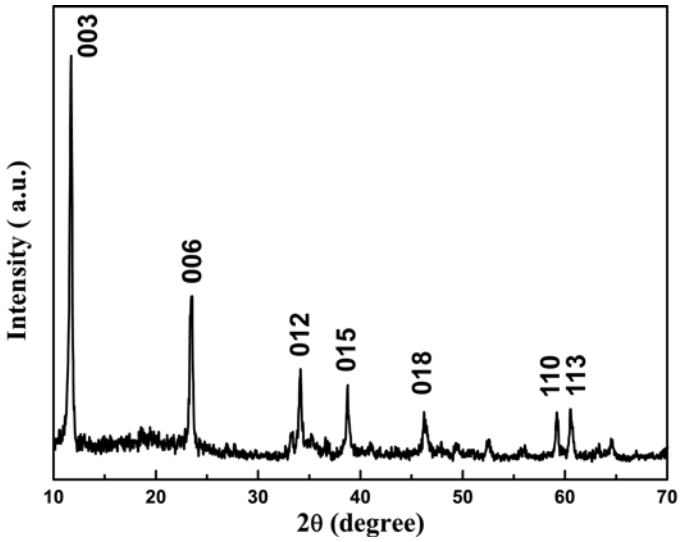

Fig. S1 XRD result of the CoFe-LDH precursor with a Co/Fe molar ratio of 5:1 showing the characteristic hydrotalcite-like reflection peaks.

Fig. S2

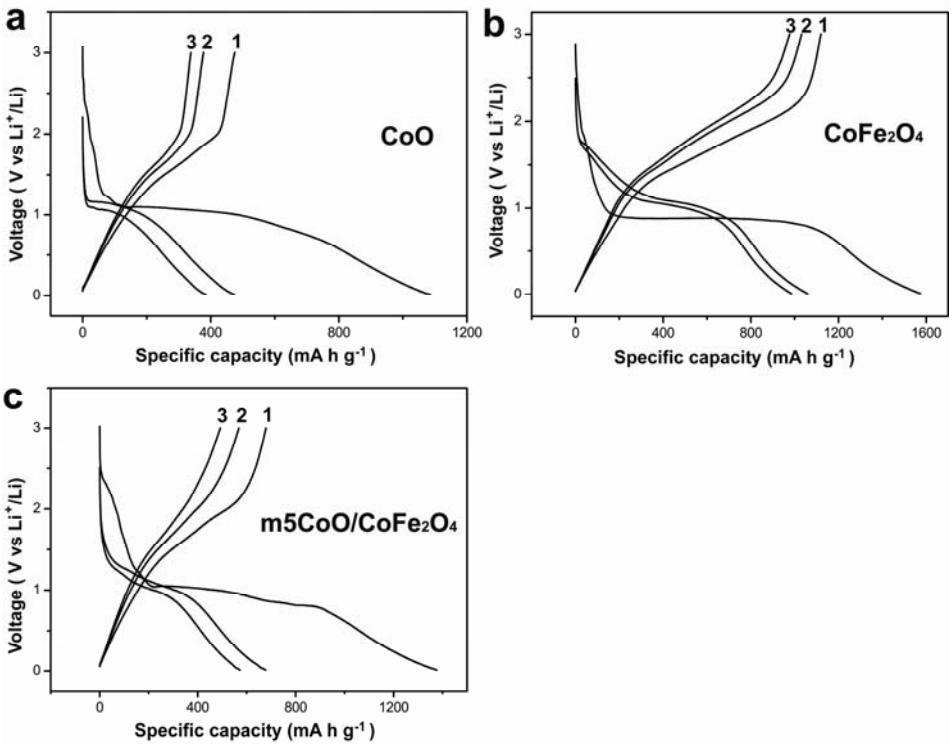

Fig. S2 The first three charge-discharge profiles of (a) CoO, (b) $CoFe_2O_4$, (c) m5CoO/$CoFe_2O_4$ cycled between 0.01–3.0 V under a current density of 100 mA g^{-1}.

Fig. S3

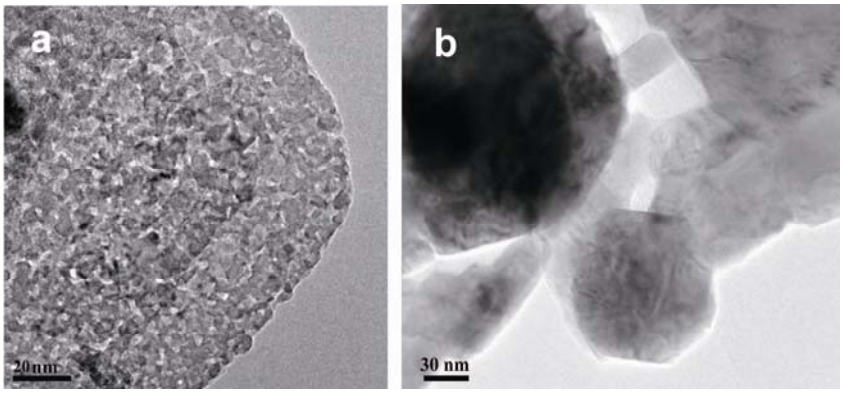

Fig. S3 Large-size TEM images of the products calcined at different temperatures: (a) at 300 °C and (b) at 700 °C.

Fig. S4

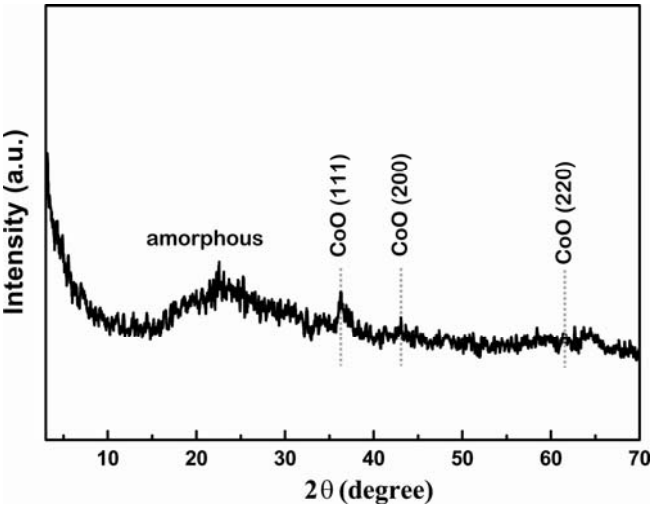

Fig. S4 XRD pattern of the product calcined at 300 °C.

Fig. S5

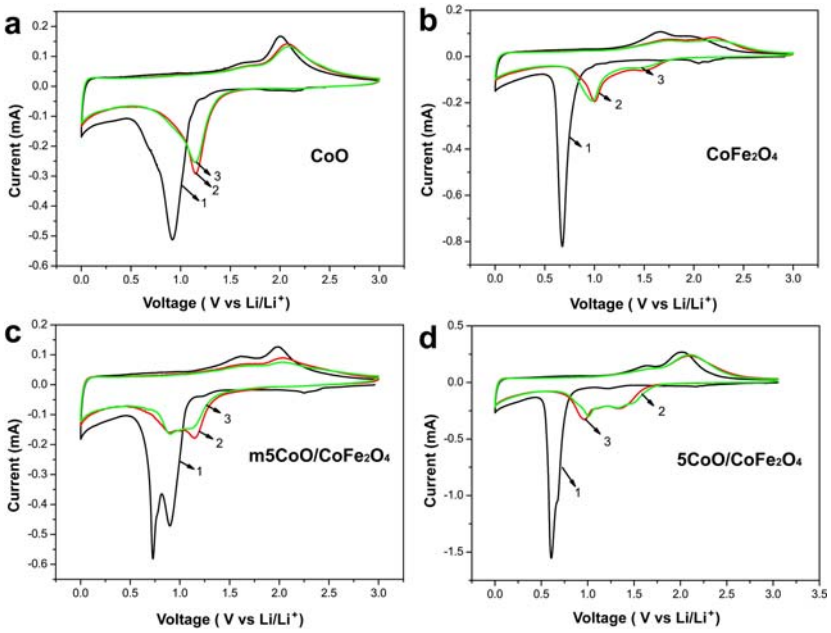

Fig. S5 The first three cyclic voltammograms of (a) CoO, (b) $CoFe_2O_4$, (c) m5CoO/$CoFe_2O_4$, (d) 5CoO/$CoFe_2O_4$ between 0–3.0V at a scan rate of 0.1 mV s^{-1}.

Cyclic voltammograms (CVs) were measured on the 5CoO/$CoFe_2O_4$ nanocomposite and the control materials upon the first three cycles at a scan rate of 0.1 mV s^{-1} between 0–3.0V. For all the electrodes, a substantial difference was observed between the first and the subsequent cycles (Fig. S5 in the ESI†). In the case of CoO (Fig. S5a in the ESI†), a large irreversible reduction peak with a maximum at about 0.9V was observed after the first cycle, and disappeared in the subsequent cycles. The change could be assigned to the formation of Li_2O and metallic Co from the reduction of CoO.

$$CoO + 2Li^+ + 2e^- \leftrightarrow Li_2O + Co$$

Compared to the initial cycle, a decrease of peak intensity could be observed with a shift of the potential (1.1V) to the positive direction in the subsequent cycles. The shift of reduction peak might be related to the pulverization of the CoO particles. Upon a anodic scan, one broad peak was recorded in the range 2.0–2.5 V corresponding to the complex phase transformation of Co^0/Co^{2+} [Refs: *Adv. Mater.* 2010, 22, E170–E192; *J. Phys. Chem. C* 2011, 115, 8400–8406].

In the case of $CoFe_2O_4$ (Fig. S5b in the ESI†), a spiky cathodic peak was present at

0.7V in the first cycle, and also disappeared in the subsequent cycles. The peak at 0.7V corresponds to the electrochemical lithium insertion reaction of Eq (1),

$$CoFe_2O_4 + 8Li^+ + 8e^- \rightarrow Co + 2Fe + 4Li_2O \quad (1)$$

$$Co + 2Fe + 4Li_2O \leftrightarrow CoO + Fe_2O_3 + 8Li \quad (2)$$

which leads to the reorganization and transformation of the $CoFe_2O_4$ nanocrystals to the nanoparticles of metallic Co, Fe, and Li_2O, and the reactions of the alkyl carbonates in electrolyte at electrode/electrolyte interphase (*Electrochim. Acta*, 2010, *55*, 4594–4598). From the second cycle, two cathodic peaks located at 1.0 and 1.6V were associated with the reversible reductive reaction of Fe_2O_3 and CoO (Eq 2). Meanwhile, two broad anodic peaks were visible at around 1.7 and 2.0V in the first cycle and shifted to around 1.8 and 2.2V, which might be attributed to the oxidation of the metallic Fe and Co to Fe^{3+} and Co^{2+}, respectively.

In contrast, in the case of the nanocomposite (Fig. S5d in the ESI†), the CV curve of $5CoO/CoFe_2O_4$ was distinctly different from those of CoO, $CoFe_2O_4$ and the mixture of $m5CoO/CoFe_2O_4$. In the first cycle, a large irreversible reduction peak was observed for $5CoO/CoFe_2O_4$ with a maximum at about 0.6V, slightly lower than those of the $m5CoO/CoFe_2O_4$ with two divided peaks at 0.7V and 0.9V that correspond to the first irreversible reduction peaks of $CoFe_2O_4$ (0.7V) and CoO (0.9V), respectively (Fig. S5c in the ESI†). Also, two board oxidation peaks at about 1.6 and 2.0V were resolved, corresponding to the phase transformation from metallic Co to CoO. From the second cycle, two board cathodic peaks between 1.0–1.6V can be attributed to the reduction of Fe_2O_3 and CoO, and two board anodic peaks between 1.6–2.1V to the oxidation of metallic Co and Fe. The CV results of all the materials clearly suggest that during the Li insertion and deinsertion, $5CoO/CoFe_2O_4$ composite exhibited almost the combined electrochemical reaction of CoO and $CoFe_2O_4$, but a slightly different from the mixture of $m5CoO/CoFe_2O_4$ (Fig. S5c in the ESI†), possibly owing to the attractive feature of the synergistic effect of CoO and $CoFe_2O_4$ of the nanocomposite.

Fig. S6

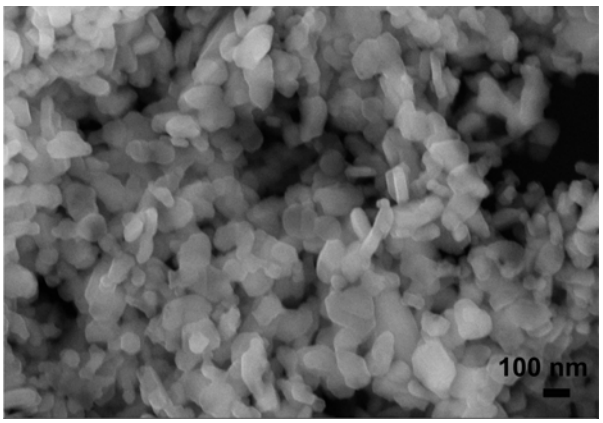

Fig. S6 SEM image of the $3CoO/CoFe_2O_4$ nanocomposite derived from the CoFe-LDH precursor with a Co/Fe molar ratio of 2:1.

Fig. S7

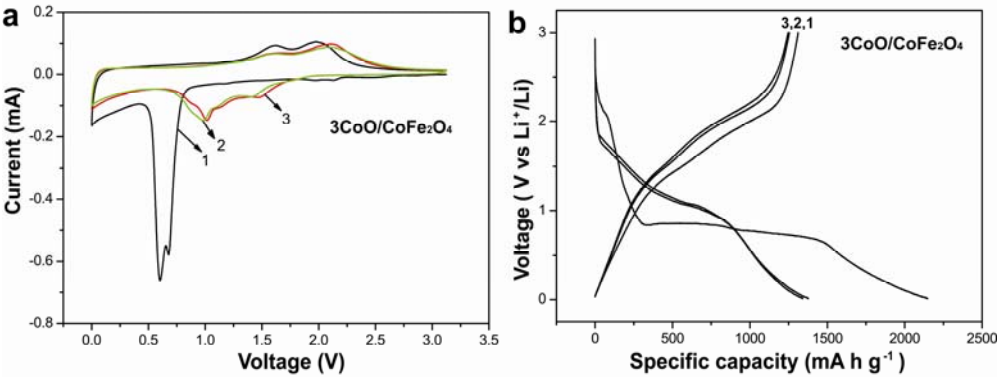

Fig. S7 The $3CoO/CoFe_2O_4$ nanocomposite: (a) the first three cyclic voltammograms between 0–3.0V at a scan rate of 0.1 mV s^{-1}, and (b) the first charge-discharge profiles between 0.01–3.0 V under a current density of 100 mA g^{-1}.

Fig. S8

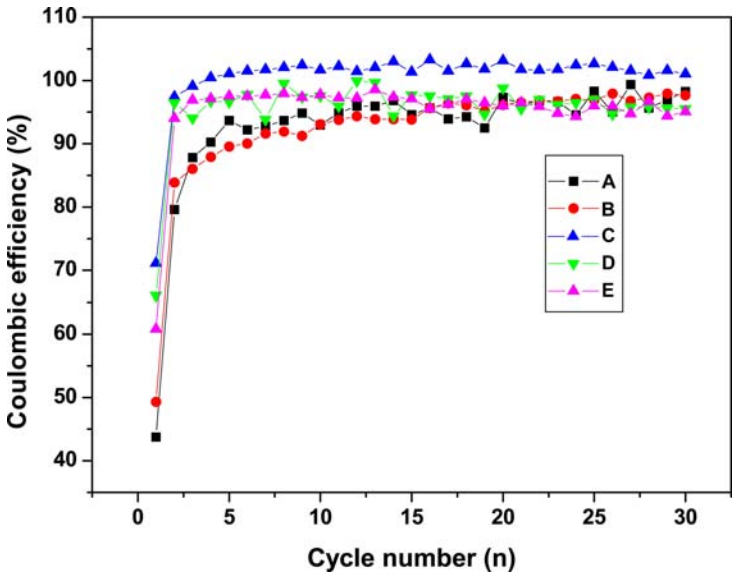

Fig. S8 Coulombic efficiencies of the electrodes. (A) CoO, (B) m5CoO/$CoFe_2O_4$, (C) $CoFe_2O_4$, (D) 5CoO/$CoFe_2O_4$, and (E) 3CoO/$CoFe_2O_4$.